

# Remote sensing observations of phytoplankton increases triggered by successive typhoons

Lei HUANG<sup>1,2</sup>, Hui ZHAO (✉)<sup>1</sup>, Jiayi PAN<sup>2,3,4</sup>, Adam DEVLIN<sup>5</sup>

<sup>1</sup> College of Ocean and Meteorology, Guangdong Ocean University, Zhanjiang 524088, China

<sup>2</sup> Institute of Space and Earth Information Science, The Chinese University of Hong Kong, Hong Kong, China

<sup>3</sup> Shenzhen Research Institute, The Chinese University of Hong Kong, Shenzhen 518057, China

<sup>4</sup> College of Marine Science, Nanjing University of Information Science and Technology, Nanjing 210044, China

<sup>5</sup> Department of Civil and Environmental Engineering, Portland State University, Portland, OR 97207, USA

© Higher Education Press and Springer-Verlag Berlin Heidelberg 2016

**Abstract** Phytoplankton blooms in the Western North Pacific, triggered by two successive typhoons with different intensities and translation speeds under different pre-existing oceanic conditions, were observed and analyzed using remotely sensed chlorophyll-a (Chl-a), sea surface temperature (SST), and sea surface height anomaly (SSHA) data, as well as typhoon parameters and CTD (conductivity, temperature, and depth) profiles. Typhoon Sinlaku, with relatively weaker intensity and slower translation speed, induced a stronger phytoplankton bloom than Jangmi with stronger intensity and faster translation speed ( $\text{Chl-a} > 0.18 \text{ mg} \cdot \text{m}^{-3}$  versus  $\text{Chl-a} < 0.15 \text{ mg} \cdot \text{m}^{-3}$ ) east of Taiwan Island. Translation speed may be one of the important mechanisms that affect phytoplankton blooms in the study area. Pre-existing cyclonic circulations provided a relatively unstable thermodynamic structure for Sinlaku, and therefore cold water with rich nutrients could be brought up easily. The mixed-layer deepening caused by Typhoon Sinlaku, which occurred first, could have triggered an unfavorable condition for the phytoplankton bloom induced by Typhoon Jangmi which followed afterwards. The sea surface temperature cooling by Jangmi was suppressed due to the presence of the thick upper-ocean mixed-layer, which prevented the deeper cold water from being entrained into the upper-ocean mixed layer, leading to a weaker phytoplankton augment. The present study suggests that both wind (including typhoon translation speed and intensity) and pre-existing conditions (e.g., mixed-layer depths, eddies, and nutrients) play important roles in the strong phytoplankton bloom, and are responsible for the stronger phytoplankton bloom after Sinlaku's passage

than that after Jangmi's passage. A new typhoon-influencing parameter is introduced that combines the effects of the typhoon forcing (including the typhoon intensity and translation speed) and the oceanic pre-condition. This parameter shows that the forcing effect of Sinlaku was stronger than that of Jangmi.

**Keywords** typhoon, mixed-layer depth, phytoplankton bloom, Northwest Pacific Ocean, upwelling

## 1 Introduction

Typhoons are systems of severe weather which occur frequently over the tropical western Pacific Ocean, exerting dramatic effects on the upper ocean dynamics. There are over 15 typhoons or tropical storms occurring annually on average in the western Pacific Ocean which may cause sea surface cooling and phytoplankton blooms along their paths through a series of physical processes including mixing, entrainment, upwelling, etc. (Chen et al., 2003; Lin et al., 2003; Liu et al., 2010; Zheng and Tang, 2007; Zhao et al., 2008, 2013). Typhoons play an important role in enhancing chlorophyll-a (Chl-a) and causing phytoplankton blooms, contributing 20%–30% of the annual new primary production in the South China Sea (Lin et al., 2003). Phytoplankton blooms (Babin et al., 2004; Zhao et al., 2008) induced by typhoon forcing also depend on the typhoon translation speed and intensity in addition to pre-typhoon mixed-layer depth and stratification. In general, strong typhoons may exert strong forcing on a large area of the ocean surface, producing strong vertical mixing and entrainments and uplifting cold and nutrient-rich water to the sea surface. Slow-moving typhoons can enhance both cooling of the surface mixed-layer and phytoplankton biomass production due to their

long forcing time.

Mixed-layer depth is an important factor influencing the upper ocean mixing characteristics under strong typhoon winds (Pan and Sun, 2013; Lü et al., 2010). The pre-existing oceanic circulations may alter the mixed-layer depth (Zheng et al., 2008, 2010). Cyclonic eddies provide a relatively favorable thermodynamic structure, uplift cold water, and thin the mixed-layer (Tsai et al., 2008; Zheng et al., 2008), while anti-cyclonic warm eddies push the isotherms downward and thicken mixed layers. The presence of a thicker mixed-layer in the warm eddy prevents the deep cold water from being entrained into the upper ocean mixed-layer (Lin et al., 2005). Therefore, the initial conditions in the ocean may influence the turbulent mixing and entrainment driven by strong typhoon winds, leading to different scenarios of phytoplankton blooms and primary productivity.

In this study, we explore phytoplankton blooms induced by two successive typhoons, and clarify the roles of different typhoon properties and oceanic pre-existing conditions on phytoplankton blooms. According to typhoon data and the Saffir-Simpson typhoon-hurricane scale<sup>1)</sup>, Sinlaku (Fig. 1(a)) originated from a tropical depression in the northwestern Pacific (127.60°E, 15.80°N) at 12:00 UTC on 07 September 2008 and was strengthened to a category 4 typhoon with a maximum sustained wind (MSW) speed of 60 m·s<sup>-1</sup> when it appeared east of Taiwan Island at 00:00 UTC on 11 September, with a slow mean translation speed of 2.8 m·s<sup>-1</sup>. Jangmi was a category 5 typhoon (Fig. 1(b)), which originated from a tropical depression in the northwestern Pacific (125.70°E,

16.70°N) at 12:00 UTC on 23 September 2008. When Jangmi arrived east of Taiwan Island at 06:00 UTC on 27 September, its MSW speed was 67 m·s<sup>-1</sup> (typhoon level), with a fast mean translation speed of 4.2 m·s<sup>-1</sup>. These two typhoons influenced almost the same area east of Taiwan Island with similar paths. However, the phytoplankton blooms they induced were much different.

## 2 Data and methodology

The typhoon data used in this study were obtained from the Unisys Weather website<sup>1)</sup>, which incorporate the best hurricane tracks from the Joint Typhoon Warning Center in the USA. Daily sea surface temperature (SST) data (TMI\_AMSRE; www.ssmi.com) were derived from the Tropical Rain Measuring Mission (TRMM), Microwave Imager (TMI), and the Advanced Microwave Scanning Radiometer-EOS (AMSR-E) with a spatial resolution of 0.25° by 0.25°. Sea surface height anomalies (SSHA) are a merged product derived from TOPEX/Poseidon, Jason-1, ERS-1/2, and ENVISAT altimeter data, available on the website of the Archiving Validation and Interpretation of Satellite Data in Oceanography (AVISO) with a 0.25° spatial resolution and a 7-day temporal interval. Sea-surface wind speed is obtained from the daily Quick Scatterometer (QuikScat) data provided by the Remote Sensing Systems in Santa Rosa, California<sup>2)</sup>. We used these data to calculate wind stress and wind-induced Ekman pumping velocity (EPV) (Zheng and Tang, 2007; Zhang et al., 2014). Daily merged Chl-a products (from

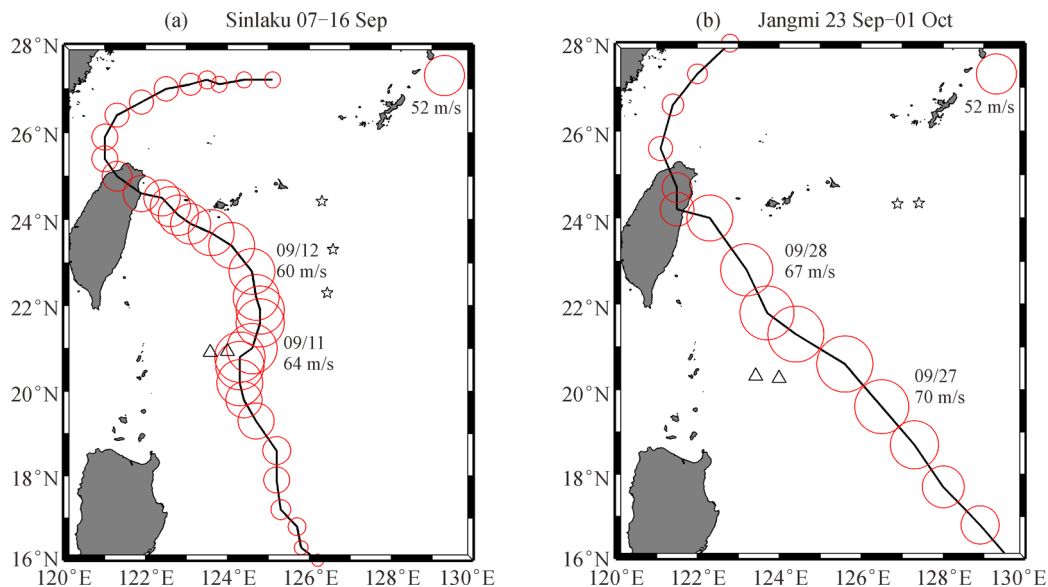


**Fig. 1** Track and intensity of typhoons (a) Sinlaku (07–16 September 2008) and (b) Jangmi (23 September–01 October 2008) in the western North Pacific (WNP).

1) [http://weather.unisys.com/hurricane/w\\_pacific/](http://weather.unisys.com/hurricane/w_pacific/)

2) <http://www.remss.com/>

SeaWiFS, MERIS, MODIS and VIIRS) with 4 km resolution were downloaded from Globcolor<sup>1)</sup>. The GlobColour project started in 2005 as an ESA Data User Element (DUE) project to provide a continuous data set of merged Level 3 Ocean Colour products. This data were also used to calculate time series of Chl-a, averaged daily. Incorporation of SSHA and microwave SST enables a comparison of upper ocean responses to a typhoon under different typhoon scenarios and pre-typhoon oceanic conditions.

Using the World Ocean Atlas climatology of 2009 (WOA 09)<sup>2)</sup>, we produced the climatological profile of temperature for September by averaging over the offshore box (Fig. 2) to indicate the typical vertical distribution of temperature. CTD profile data were downloaded from the website of the global Argo profile array<sup>3)</sup>, with a vertical resolution of 5 m in the upper 100 m. The data (depicted by five pentacles and four triangles in Fig. 1) were used to plot the temperature-depth profiles and indicate vertical changes to the upper ocean thermal structure in the offshore typhoon-induced region. Finally, in order to

investigate quantitative variation of Chl-a and other oceanic conditions, time series of Chl-a and other variables were produced and discussed, based on the average of the selected sampling region.

### 3 Results

#### 3.1 Chlorophyll-a

Satellite-derived Chl-a concentration (Fig. 2(a)) averaged for 05–12 September 2009 was generally low ( $\text{Chl-a} < 0.11 \text{ mg} \cdot \text{m}^{-3}$ ) prior to the Sinlaku's arrival in the study area (also averaged over  $122.5^{\circ}$ – $125^{\circ}\text{E}$ ,  $21^{\circ}$ – $24^{\circ}\text{N}$ , the box in Figs. 2(b) and 2(c)). Relatively high Chl-a concentration ( $\text{Chl-a} > 0.20 \text{ mg} \cdot \text{m}^{-3}$ ) was confined to the coastal zones (within about 20 km from the coastlines). However, Chl-a concentration clearly changed one week after the two typhoons' passed. There was a significant bloom region offshore, east of Taiwan Island along Sinlaku's track (7–16 September). The offshore Chl-a

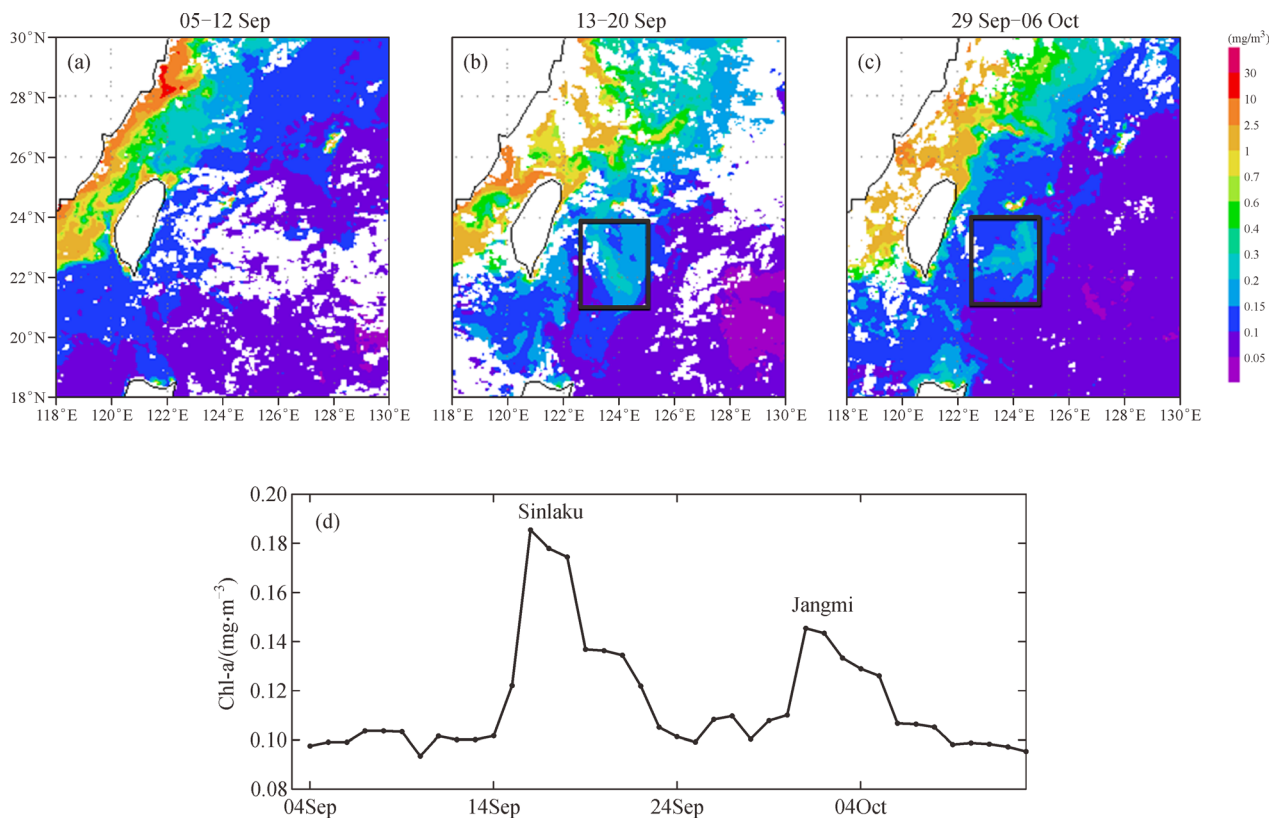


**Fig. 2** (a) Chlorophyll-a (Chl-a) concentration ( $\text{mg} \cdot \text{m}^{-3}$ ) before Typhoon Sinlaku; Chl-a concentration ( $\text{mg} \cdot \text{m}^{-3}$ ) after Typhoon (b) Sinlaku and (c) Jangmi; (d) time series of daily Chl-a concentration averaged over an offshore region ( $122.5^{\circ}$ – $125^{\circ}\text{E}$ ,  $21^{\circ}$ – $24^{\circ}\text{N}$ ) shown as the box in (b) and (c).

1) <http://hermes.acri.fr/>

2) <http://www.nodc.noaa.gov/OC5/WOA09/>

3) <http://www.aoml.noaa.gov/>

concentration (Fig. 2(b)) increased from  $0.10$  to  $0.18 \text{ mg}\cdot\text{m}^{-3}$  (Fig. 2(d)) in the study area (averaged over the offshore area:  $122.5^{\circ}$ – $125^{\circ}\text{E}$ ,  $21^{\circ}$ – $24^{\circ}\text{N}$ , the box in Figs. 2(b) and 2(c)). Then, the Chl-a concentration decreased to a level of  $0.10$ – $0.11 \text{ mg}\cdot\text{m}^{-3}$  (Fig. 2(d)) two weeks before Typhoon Jangmi appeared in the offshore Chl-a bloom area. Along Jangmi's track (23 September–01 October), the offshore Chl-a concentration (Fig. 2(c)) increased slightly only from  $0.11$  to  $0.14 \text{ mg}\cdot\text{m}^{-3}$  (Fig. 2(d)) in the study area, less than that induced by Sinlaku.

### 3.2 Sea surface temperature

Before the passage of Sinlaku on 11 September 2008, the study area was occupied by warm water. The SST averaged over the offshore region ( $122.5^{\circ}$ – $125^{\circ}\text{E}$ ,  $21^{\circ}$ – $24^{\circ}\text{N}$ ) and Fig. 3(a) indicated that high temperature water ( $\text{SST} > 29^{\circ}\text{C}$ ) appeared in the region before Sinlaku and Jangmi passed. The SST decrease was evident after Sinlaku's and Jangmi's passages. There was a low SST patch ( $\text{SST} < 26^{\circ}\text{C}$ ) near Sinlaku's track (Fig. 3(b)) east of Taiwan Island, roughly a decrease of  $3^{\circ}\text{C}$ – $4^{\circ}\text{C}$  on September 13 (Fig. 3(d)). However, the SST drop induced by Jangmi was only  $\sim 1^{\circ}\text{C}$  on September 30 (Fig. 3(d)). The area of the low SST patch caused by Sinlaku was also larger than that caused by Jangmi.

### 3.3 Sea surface height anomaly

Under the forcing of the strong typhoon winds, Ekman pumping lifts the lower layer water and the divergent flow at the surface may decrease sea surface height (Price, 1981; Wei et al., 2003; Hu and Hiroshi, 2004). Figure 4 shows the sea surface height anomaly (SSHA) from 03 September to 07 October 2008. Before the arrival of Typhoon Sinlaku, there was a cyclonic eddy in the study area (Fig. 4(a)). From May to September, intense solar radiance heats the surface water, and therefore, the sea surface is usually covered by the warm water (Lin et al., 2003). Thus, the SST drop associated with the cyclonic eddy was not evident. When Sinlaku arrived in the area, the SSHA decreased by about 10 cm (Fig. 4(b)), and the cold, cyclonic, mesoscale eddy was strengthened. After Jangmi's passage, the cold mesoscale eddy was further enhanced (Fig. 4(c)) with a SSHA decrease of about 20 cm, but the diameter of the eddy decreased (Figs. 4(c) and 4(d)). In contrast, the warm eddy on the right was strengthened substantially (Figs. 4(c) and 4(d)). The area of the negative SSHA patch caused by Jangmi was smaller than that caused by Sinlaku (Figs. 4(b), 4(c), and 4(d)), consistent with the SST patterns (Fig. 3). The response of sea surface height to the typhoon forcing was strong when Sinlaku passed, and the SSHA decreased significantly.

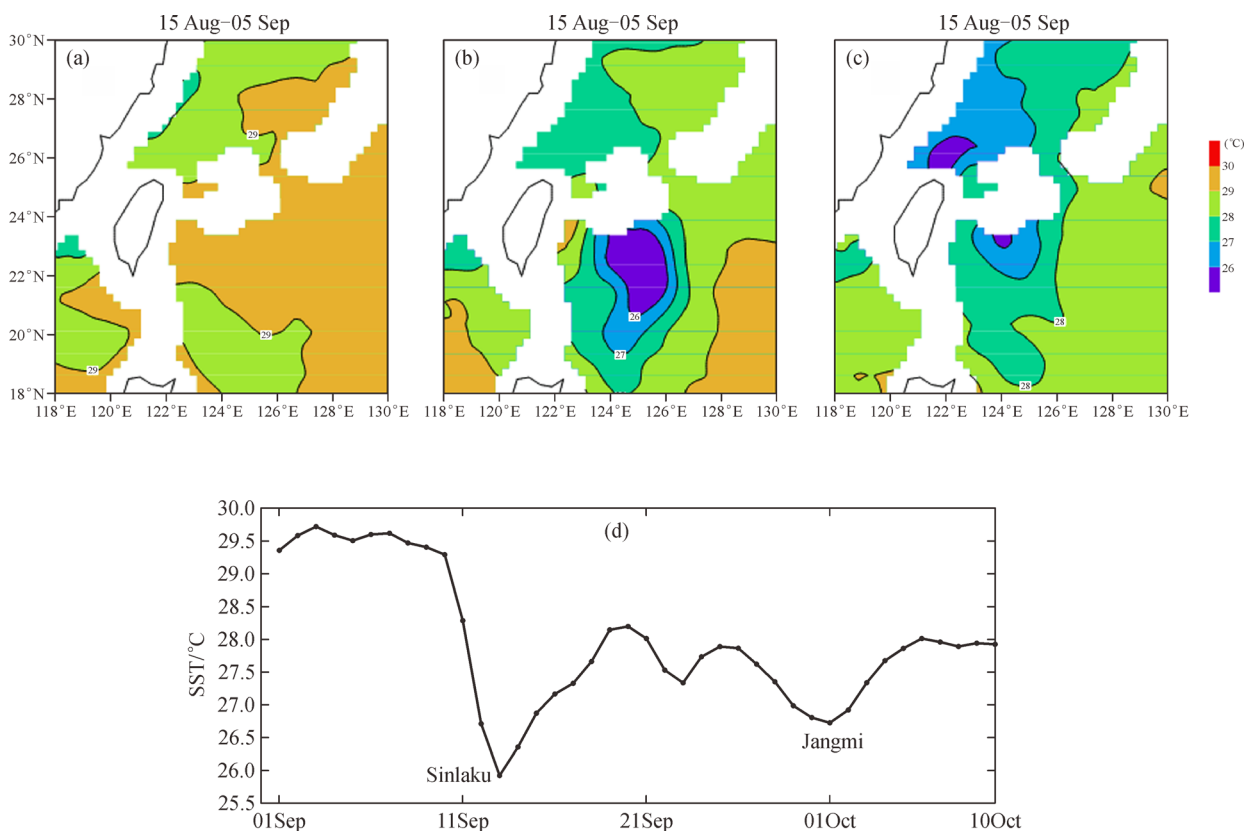


**Fig. 3** (a) SST before Typhoon Sinlaku; SST after Typhoon (b) Sinlaku and (c) Jangmi; (d) time series of SST averaged over the offshore region ( $122.5^{\circ}$ – $125^{\circ}\text{E}$ ,  $21^{\circ}$ – $24^{\circ}\text{N}$ ) shown as the box in Fig. 2(b) and 2(c).

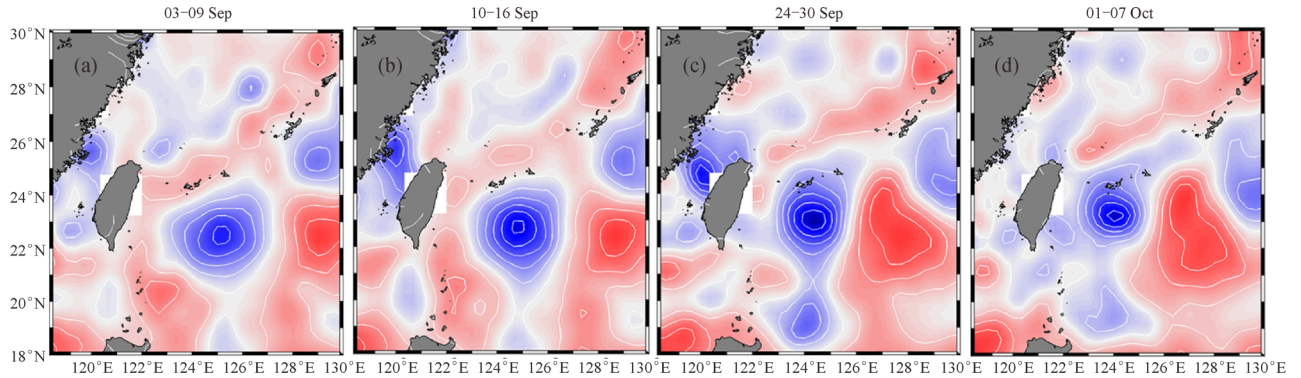


Fig. 4 SSHA (cm) from September to early October, 2008.

After Jangmi, however, the cold eddy was not so obvious compared with that induced by Sinlaku.

## 4 Analysis and discussion

### 4.1 Typhoon intensity and translation speed

The Ekman pumping velocity (EPV,  $W_e$ ) revealing the upwelling intensity is written as:

$$W_e = \text{curl}_z \left( \frac{\tau}{\rho_w f} \right), \quad (1)$$

where  $\rho_w$  is the seawater density,  $f$  is the Coriolis parameter, and  $\tau$  is the wind stress on the ocean surface. The wind stress is calculated with (Stewart, 2008)

$$\tau = \rho_a C_D |U_{10}| U_{10}, \quad (2)$$

where  $\rho_a = 1.3 \text{ kg} \cdot \text{m}^{-3}$  is the air density,  $C_D = 10^{-3}(0.6 + 0.07U_{10})$  is the drag coefficient, and  $U_{10}$  is the wind speed at 10 m above the sea surface from the QuikScat wind product. The spatially averaged EPV over the offshore area ( $122.5^\circ\text{--}125^\circ\text{E}$ ,  $21^\circ\text{--}24^\circ\text{N}$ ) is shown in Fig. 5 for Sinlaku (a) and for Jangmi (b). Figure 5 indicates that though the maximum daily EPV induced by Sinlaku was weaker than

that induced by Jangmi ( $1.7 \times 10^{-4} \text{ m} \cdot \text{s}^{-1}$  versus  $1.9 \times 10^{-4} \text{ m} \cdot \text{s}^{-1}$ ), its temporal integral over the typhoon forcing period (10 to 12 September 2008) reached 28.3 m, higher than that of Jangmi, 16.1 m (integral of the EPV over 27 to 29 September 2008).

Sinlaku induced a more intense phytoplankton bloom (Fig. 2(b) and 2(d)) than Jangmi (Fig. 2(c) and 2(d)). The result suggests that the translation speed of a typhoon is an important factor affecting phytoplankton blooms. The slower moving Sinlaku ( $2.8 \text{ m} \cdot \text{s}^{-1}$ ) enhanced its effect on upper-ocean cooling and nutrient injection into the surface layer, whereas Jangmi with a faster translation speed ( $4.2 \text{ m} \cdot \text{s}^{-1}$ ), might not have such strong effects on the upper ocean due to its shorter forcing time. Therefore, the cumulative entrainment and upwelling could be more significant for the relatively slow and weak Sinlaku.

### 4.2 In situ observation

We use conductivity-temperature-depth (CTD) data of nine stations around the two typhoon tracks near the phytoplankton bloom region. On the west side, there were four profiles measured on 01 September, 11 September, 21 September, and 01 October by Argo float 40947. On the east side, there were five profiles measured on 01 September, 11 September, 16 September, 21 September,

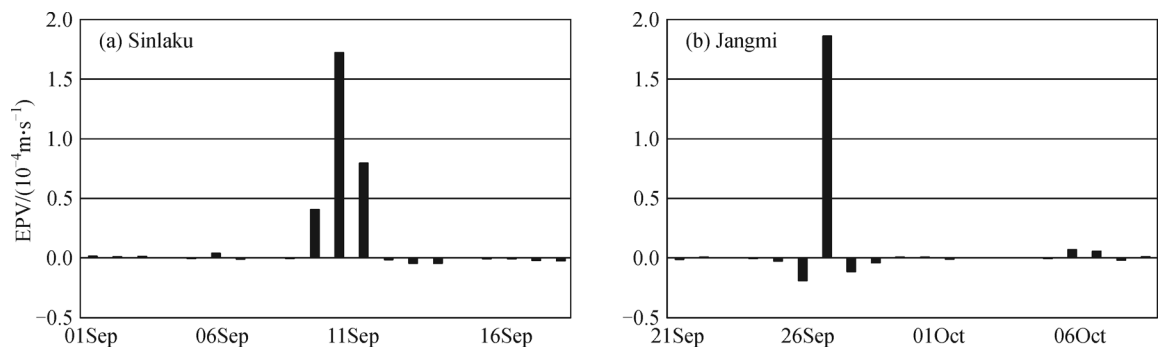


Fig. 5 Time series of Ekman pumping velocity ( $10^{-4} \text{ m} \cdot \text{s}^{-1}$ ) during (a) Sinlaku and (b) Jangmi averaged over the offshore area ( $122.5^\circ\text{--}125^\circ\text{E}$ ,  $21^\circ\text{--}24^\circ\text{N}$ ) for both Sinlaku and Jangmi.

and 01 October by Argo float 80052. The locations of these profiles are illustrated in Fig. 1 and listed in Table 1. On the both sides of the typhoon tracks, the temperature profiles varied substantially after Sinlaku's and Jangmi's passages. The climatological temperature profile (Fig. 6(a)) reveals that the MLD (mixed-layer depth) is 45 m. On the west side of the typhoon track, the MLD was less than 30 m with a high SST of over 29°C and weak stratification (Fig. 6(b), black dashed line), as indicated by the temperature profile before the arrival of Sinlaku on 01 September in the upper ocean, as a result of a cold eddy (Fig. 4(a)) before Sinlaku. The MLD deepened to about 60 m on 21 September after Sinlaku, and the temperature decreased substantially below the mixed-layer. After Jangmi, the MLD deepened to 70 m on October 01. On the east side of the typhoon track, the mixed-layer deepened to 60 m and 70 m after Sinlaku on 11 September and 16 September, respectively. On 21 September, the MLD was 35 m. After Jangmi's passage on October 01, the mixed-layer deepened to 55 m, less than that induced by Sinlaku. The results indicate that the upwelling and mixing induced by Sinlaku was stronger than that by Jangmi.

#### 4.3 Mixed-layer deepening and pre-existing oceanic conditions

Mixed-layer depth is an important factor influencing the upper ocean mixing characteristic under strong typhoon winds. The significant SST drop and mixed-layer deepening are associated with upper-ocean dynamical processes (mixing, upwelling, entrainment, etc.) when typhoon winds decelerated and generation of inertial-gravity waves was restricted (Pan and Sun, 2013). The *in situ* observation results (Figs. 6(b) and 6(c); Table 1) show that whether on the west side or east side, Sinlaku caused a much deeper upper ocean mixed-layer than Jangmi. The accumulation of Ekman pumping (Fig. 5) might be one of the key factors.

On the other hand, pre-existing cyclonic eddy (Fig. 4(a)) structures could provide favorable conditions for typhoon Sinlaku to induce upper ocean responses efficiently (Zheng et al., 2008). Once a typhoon approaches an area with a cyclonic eddy, sufficient surface cooling can occur. The pre-existing cyclonic circulations (Fig. 4(a)) may form a favorable thermodynamic structure, including weak stratification (Figs. 6(b) and 6(c)), observed in the upper ocean before Sinlaku's passage and cold water near the sea surface, which might enhance typhoon-induced upper ocean response. Therefore, the water could be easily uplifted through entrainment. When typhoon Sinlaku arrived to east of Taiwan Island, strong turbulent mixing and upwelling appeared, as generated by strong typhoon wind stress (Pan and Sun, 2013). Around its track, the averaged mixed-layer deepened to 70 m after Sinlaku. This thick upper-ocean mixed-layer (Figs. 6(b) and 6(c); Table 1) formed a new dynamical environment before Typhoon Jangmi reached the study area. After Jangmi arrived, the deepened mixed-layer caused by the Typhoon Sinlaku could form an unfavorable condition for the surface cooling induced by Jangmi. The sea surface temperature decrease could be suppressed (Figs. 3(c) and 3(d)) owing to the presence of the thicker upper-ocean mixed-layer (Figs. 6(b) and 6(c)), which prevents deep cold water from being entrained into the upper-ocean mixed-layer (Lin et al., 2005), leading to a weaker phytoplankton bloom (Figs. 2(c) and 2(d)).

In the upper ocean, light conditions and nutrients play important roles in the changes of the Chl-a concentration (Yentsch, 1965; Furuya, 1990). The vertical distributions of Chl-a concentration are determined by their spatial structures (Gong et al., 2012). A bell-shaped vertical profile of Chl-a concentration, conventionally referred to as a subsurface chlorophyll maximum (SCM) phenomenon, has frequently been observed in stratified oceans. Therefore, Chl-a generally maximizes in the subsurface layer of the stratified water columns of the offshore deep

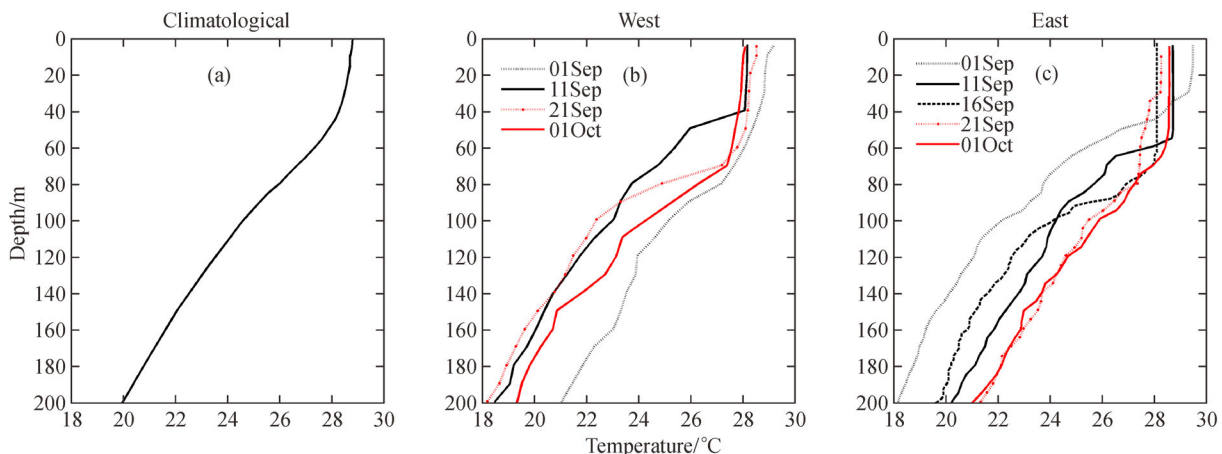


**Fig. 6** (a) Vertical profiles of the climatological temperature (°C) in September, CTD temperature profiles on the (b) west side and (c) east side of the typhoon tracks.

**Table 1** The CTD time and locations, sea surface cooling at the locations, and mixed-layer deepening estimated based on the CTD temperature profiles

| No. | Time   | Location          | $T/^\circ\text{C}$ | $\Delta T/^\circ\text{C}$ | MLD/m | $\Delta\text{MLD/m}$ |
|-----|--------|-------------------|--------------------|---------------------------|-------|----------------------|
| 1   | 1-Sep  | 20.91°N, 123.58°E | 29.2               | -----                     | 30    | -----                |
| 2   | 11-Sep | 20.93°N, 124.00°E | 28.2               | -1                        | 42    | 12                   |
| 3   | 21-Sep | 20.27°N, 123.91°E | 28.5               | -----                     | 60    | -----                |
| 4   | 1-Oct  | 20.23°N, 123.43°E | 28.1               | -0.4                      | 70    | 10                   |
| 5   | 1-Sep  | 22.30°N, 126.44°E | 29.5               | -----                     | 30    | -----                |
| 6   | 11-Sep | 23.31°N, 126.58°E | 28.7               | -0.8                      | 60    | 30                   |
| 7   | 16-Sep | 24.42°N, 126.31°E | 28.2               | -1.3                      | 70    | 40                   |
| 8   | 21-Sep | 24.33°N, 126.89°E | 28.3               | -----                     | 35    | -----                |
| 9   | 1-Oct  | 24.35°N, 127.41°E | 28.6               | 0.3                       | 55    | 20                   |

$T$ : sea surface temperature from the Argo profiles,  $\Delta T$ : sea surface cooling, MLD: mixed-layer depth from the Argo profiles, and  $\Delta\text{MLD}$ : mixed-layer deepening.

ocean where there are rich nutrients. The subsurface maxima of Chl-a (Gong et al., 2015) are usually produced in certain regions of the water column where two opposing resource (light and nutrient) gradients combined with turbulent mixing are amenable for survival of phytoplankton. Chen et al. (2003) also found the summer SCM in the offshore region east of Taiwan Island, where the Chl-a is at a maximum at a depth of 100 m. Therefore, in the present study, light will not be a limiting factor in the mixed-layer deepened by the two typhoons, but nutrients had been depleted after Sinlaku's passage in the upper ocean. As the results of *in situ* observations (Figs. 6(b) and 6(c)), the mixed-layer depth induced by Jangmi was limited, and the increase in Chl-a concentration was weakened after Jangmi.

#### 4.4 A new typhoon-influencing parameter

In order to determine the combined effect of wind and pre-existing oceanic conditions, we introduce a new typhoon-influencing parameter, given by

$$C = \frac{\int_{t_1}^{t_2} W_e dt}{\text{MLD}}, \quad (3)$$

where MLD is the mixed-layer depth before typhoon,  $t_1$  and  $t_2$  represent the beginning and ending time of the period when the typhoon passed over the study area. In Eq. (3), the temporal integral of the EPV ( $W_e$ ) and MLD represent positive and negative effects on the phytoplankton blooms, respectively. For Sinlaku, the temporal integral of EPV is 28.3 m and averaged MLD before the typhoon is 30 m, so that the typhoon-influencing parameter  $C$  derived from Eq. (3) is 0.94. For Jangmi, the temporal integral of EPV is 16.1 m and the averaged MLD before the typhoon is 42.5 m, in this case, the parameter  $C$  is calculated as 0.38. This indicates that the forcing effect of Sinlaku was much stronger than that of Jangmi.

## 5 Summary

With remote sensing data, we observed two Chl-a blooms east of Taiwan Island after the passages of Sinlaku and Jangmi. These two phytoplankton blooms were closely related to the typhoon intensity and translation speed, as well as the pre-existing oceanic conditions (e.g., mixed-layer depth, eddies, nutrients). The combination of these factors may control the upper ocean dynamical responses to the typhoon forcing. Due to a longer forcing time, the slower moving and weaker Typhoon Sinlaku induced higher phytoplankton blooms than the faster moving and stronger Jangmi. The pre-existing cyclonic circulations provided a relatively favorable thermodynamic structure for Sinlaku, and therefore, the cold and nutrient-rich water would be lifted up easily, enhancing both cooling of the surface mixed-layer and phytoplankton biomass production. After Jangmi with faster translation speed arrived in the study area, sea surface temperature cooling was suppressed owing to the presence of the thick upper-ocean mixed-layer caused by Sinlaku, which hampered the deep cold water being entrained into the upper-ocean mixed-layer, leading to a weaker phytoplankton bloom. A typhoon-influencing parameter is introduced that combines the effects of the typhoon forcing (including the typhoon intensity and translation speed) and the oceanic precondition. The typhoon-influencing parameter shows that the forcing effect of Sinlaku was much stronger than that of Jangmi.

**Acknowledgements** The present research is supported by 1) the Foundation for Distinguished Young Teacher in Higher Education of Guangdong (YQ2013092), 2) the Strategic Priority Research Program of the Chinese Academy of Sciences (XDA11020305, CDA11010301), 3) Project of Enhancing School With Innovation of Guangdong Ocean University, and 4) the National Natural Science Foundation of China (Grant Nos. 41376125, 41006070, and 41376035). This work is also supported by the General Research Fund of Hong Kong Research Grants Council (RGC) under grants CUHK 402912 and 403113, the Hong Kong Innovation and Technology

Fund under the grants of ITS/321/13, and the direct grants of the Chinese University of Hong Kong. We thank GlobColor's Working Group for providing merged Chlorophyll-a data, Remote Sensing Systems for TMI-AMSRE sea-surface temperature and QuikScat wind vector data, the Colorado Center for Astrodynamics Research (CCAR) Altimeter Data Research Group for sea-level anomaly data. The authors are very grateful to the anonymous reviewers for their valuable comments and suggestions.

## References

- Babin S M, Carton J A, Dickey T D, Wiggert J D (2004). Satellite evidence of hurricane induced phytoplankton blooms in an oceanic desert. *J Geophys Res*, 109(C3): 1978–2012
- Chen C T A, Liu C T, Chuang W S, Yang Y J, Shiah F K, Tang T Y, Chung S W (2003). Enhanced buoyancy and hence upwelling of subsurface Kuroshio waters after a typhoon in the southern East China Sea. *J Mar Syst*, 42(1–2): 65–79
- Furuya K (1990). Subsurface chlorophyll maximum in the tropical and subtropical western Pacific Ocean: vertical profiles of phytoplankton biomass and its relationship with chlorophylla and particulate organic carbon. *Mar Biol*, 107(3): 529–539
- Gong X, Shi J, Gao H W (2012). Subsurface chlorophyll maximum in ocean: its characteristics and influencing factors. *Adv Earth Sci*, 27(5): 539–548 (in Chinese)
- Gong X, Shi J, Gao H W, Yao X H (2015). Steady-state solutions for subsurface chlorophyll maximum in stratified water columns with a bell-shaped vertical profile of chlorophyll. *Biogeosciences*, 12(4): 905–919
- Hu J Y, Hiroshi K (2004). Detection of cyclonic eddy generated by looping tropical cyclone in the northern South China Sea: a case study. *Acta Oceanol Sin*, 23(2), 213–224
- Lin I I, Wu C C, Emanuel K A, Lee I H, Wu C R, Pun I F (2005). The interaction of Super typhoon Maemi (2003) with a warm ocean eddy. *Mon Weather Rev*, 133(9): 2635–2649
- Lin I, Liu W T, Wu C C, Wong G T F, Hu C, Chen Z, Liang W D, Yang Y, Liu K K (2003). New evidence for enhanced ocean primary production triggered by tropical cyclone. *Geophys Res Lett*, 30(13), doi: 10.1029/2003GL017141
- Liu G Q, He Y J, Shen H, Qiu Z F (2010). Submesoscale activity over the shelf of the northern South China Sea in summer: simulation with an embedded model. *Chinese Journal of Oceanology and Limnology*, 28: 1073–1079
- Lü H, He Y J, Shen H, Cui L M, Dou C E (2010). A new method for the estimation of oceanic mixed-layer depth using shipboard X-band radar images. *Chin J Oceanology Limnol*, 28(5): 962–967
- Pan J Y, Sun Y J (2013). Estimate of ocean mixed layer deepening after a typhoon passage over the south china sea by using satellite data. *J Phys Oceanogr*, 43(3): 498–506
- Price J F (1981). Upper ocean response to a hurricane. *J Phys Oceanogr*, 11(2): 153–175
- Stewart R H (2008). *Introduction to Physical Oceanography*. Texas: Texas A & M University, 49–50
- Tsai Y, Chern C S, Wang J (2008). The upper ocean response to a moving typhoon. *J Oceanogr*, 64(1): 115–130
- Wei Z X, Fang G H, Choi B H, Fang Y, He Y J (2003). Sea surface height and transport stream function of the South China Sea from a variable-grid global ocean circulation model. *Sci China Ser D*, 46(2): 139–148
- Yentsch C S (1965). Distribution of chlorophyll and phaeophytin in the open ocean. *Deep Sea Research and Oceanographic Abstracts*, 12(5): 653–666
- Zhang B, Perrie W, Zhang J A, Uhlhorn E W, He J Y (2014). High-resolution hurricane vector winds from C-band dual-polarization SAR observations. *J Atmos Ocean Technol*, 31(2): 272–286
- Zhao H, Han G Q, Zhang S W, Wang D X (2013). Two phytoplankton blooms near Luzon Strait generated by lingering Typhoon Parma. *J Geophys Res Biogeosci*, 118(2): 412–421
- Zhao H, Tang D L, Wang Y (2008). Comparison of phytoplankton blooms triggered by two typhoons with different intensities and translation speeds in the South China Sea. *Mar Ecol Prog Ser*, 365: 57–65
- Zheng G M, Tang D L (2007). Offshore and nearshore chlorophyll increases induced by typhoon winds and subsequent terrestrial rainwater runoff. *Mar Ecol Prog Ser*, 333: 61–74
- Zheng Z W, Ho C R, Kuo N J (2008). Importance of pre-existing oceanic conditions to upper ocean response induced by Super Typhoon Hai-Tang. *Geophys Res Lett*, 35(20): L20603
- Zheng Z W, Ho C R, Zheng Q, Lo Y T, Kuo N J, Gopalakrishnan G (2010). Effects of preexisting cyclonic eddies on upper ocean responses to Category 5 typhoons in the western North Pacific. *J Geophys Res* (1978–2012), 115(C9): C09013